Science of the Total Environment 657 (2019) 1311–1322

Contents lists available at ScienceDirect

Science of the Total Environment

journal homepage: www.elsevier.com/locate/scitotenv

Riverine carbon dioxide evasion along a high-relief watercourse derived from seasonal dynamics of the water-atmosphere gas exchange

T.R. Juhlke [a,*], R. Van Geldern [a], F. Huneau [b,c], E. Garel [b,c], S. Santoni [b,c], H. Hemmerle [a], J.A.C. Barth [a]

[a] Friedrich-Alexander-Universität Erlangen-Nürnberg (FAU), Department Geographie und Geowissenschaften, GeoZentrum Nordbayern, Schlossgarten 5, 91054 Erlangen, Germany
[b] Université de Corse Pascal Paoli, Faculté des Sciences et Techniques, Laboratoire d'Hydrogéologie, Campus Grimaldi, BP 52, F-20250 Corte, France
[c] CNRS, UMR 6134 SPE, F-20250 Corte, France

HIGHLIGHTS

- Carbon isotope values of river water indicate atmospheric CO_2 influence in winter.
- In summer, soil CO_2 was the main carbon contributor to the stream.
- Half of the main stream length is undersaturated with respect to CO_2 year-round.
- Annual main stream air-water carbon flux is 7 times higher than riverine DIC export.

GRAPHICAL ABSTRACT

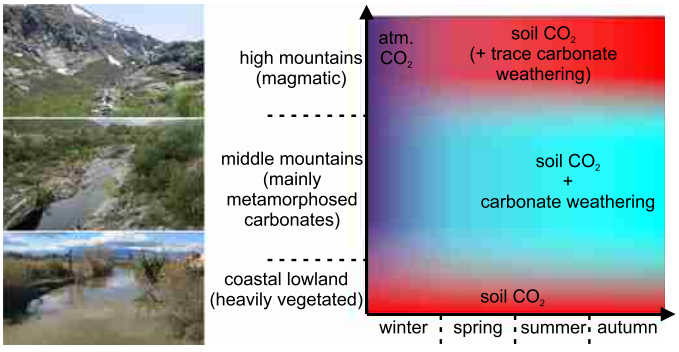

ARTICLE INFO

Article history:
Received 26 October 2018
Received in revised form 10 December 2018
Accepted 10 December 2018
Available online 11 December 2018

Editor: Damia Barcelo

Keywords:
Carbon dioxide degassing
Dissolved inorganic carbon
Stable isotopes
Carbon cycle
Western Mediterranean

ABSTRACT

The high-relief catchment of the Tavignanu River (Corsica Island, France) with an elevation range from sea level to 2622 m above sea level was investigated for its riverine carbon budget and stable carbon isotopes. Major riverine dissolved inorganic carbon (DIC or TCO_2) sources depended on seasons and sub-catchment lithology. In winter $\delta^{13}C_{DIC}$ values of −2 to −7‰ (VPDB) indicated influences of atmospheric CO_2. $\delta^{13}C_{DIC}$ values decreased gradually to values between −9 and −12‰ in July, which indicates elevated soil CO_2 contribution. An observed downstream increase in the total amount of carbon species correlated with inputs from carbonate bearing tributaries and evaporation effects in summer. Main channel partial pressure of CO_2 (pCO_2) was seasonally highly variable in the upper silicate catchment and the lower coastal plain, where summer values exceed up to six times atmospheric levels. During winter, the central section of the Tavignanu River was found to be undersaturated with respect to atmospheric CO_2 levels. The median values for main channel pCO_2 were below atmospheric levels in winter and spring and above in summer and autumn. The annual carbon flux across the air-water boundary (F_{CO_2}) along the Tavignanu River was calculated with (0.77 ± 0.24) Gg C yr^{-1}, which is about seven times higher than the riverine TCO_2 transport to the sea of about 0.11 Gg C yr^{-1}. While large sections of the river experienced year-round atmospheric CO_2 uptake or equilibrium, the river as a whole was a small but continuous net source of carbon to the atmosphere. This underlines the important, but so far not well-constrained, contributions of smaller streams and rivers to the terrestrial carbon flux and the need of incorporating them into future global carbon cycle models.

* Corresponding author.
E-mail address: tobias.juhlke@fau.de (T.R. Juhlke).

https://doi.org/10.1016/j.scitotenv.2018.12.158
0048-9697/

1. Introduction

The global carbon cycle consists of several major reservoirs including the atmosphere, terrestrial and oceanic biomass, soils, carbonate rocks, fossil hydrocarbons, and dissolved inorganic carbon (TCO_2) in oceans. These reservoirs are interconnected not by simple conduits but by pathways along which carbon can be stored or returned to other compartments (Aufdenkampe et al., 2011; Cole et al., 2007; Wehrli, 2013). One of those pathways are river systems that transport carbon from terrestrial sources to the ocean. The estimated global average of total carbon exported to the oceans is around 0.9 Pg C yr^{-1} (Battin et al., 2009; Cole et al., 2007; Meybeck, 1982; Tranvik et al., 2009; Wehrli, 2013).

Various terrestrial carbon sources feed the river systems where carbon can be transported as organic or inorganic, and dissolved or particulate species. Soil CO_2 derived from plant respiration increases the partial pressure of CO_2 (pCO_2) in soil air and consequently raises the amount of dissolved carbon species in soil water (Dever et al., 1983; Salomons and Mook, 1986). TCO_2 is then transported from the soils to the rivers via underground flow (soil water or groundwater) and surface runoff (Barth et al., 2003; Hélie et al., 2002; Raymond and Bauer, 2001; Raymond et al., 2004). On its way, the CO_2 rich waters can contribute to chemical weathering of silicate and carbonate rocks and further increase the TCO_2 content (Amiotte Suchet and Probst, 1995; Aucour et al., 1999; Hagedorn and Cartwright, 2009; Kanduč et al., 2012; Kanduč et al., 2007; Lee et al., 2017; Sharp et al., 1995; Telmer and Veizer, 1999). Physical erosion of flowing water (Aucour et al., 1999) and atmospheric input of carbonate aerosols (Loÿe-Pilot et al., 1986; Mamane et al., 1987) are further sources of TCO_2.

For some time, it was assumed in models of the global carbon cycle that rivers act as passive pipes and the simple one-way transport of carbon from land to sea was the only significant process attributed to them (Cole et al., 2007). Newer studies revealed that during the downstream course, further processes alter and even export TCO_2 from river water, so that only a fraction of the original terrestrial TCO_2 input eventually reaches the ocean (Aufdenkampe et al., 2011; Wehrli, 2013). Various in-river processes induced by the biosphere (photosynthesis, respiration and biomass decay), and water-rock interactions (especially dissolution of carbonates) are known to influence the river's TCO_2 chemistry (Barth and Veizer, 1999; Pawellek and Veizer, 1994; Raymond and Bauer, 2001; Raymond et al., 2004; Telmer and Veizer, 1999; Yang et al., 1996).

For pCO_2 values in river water lower than atmospheric levels, direct invasion of atmospheric CO_2 is possible (Raymond et al., 2000; Wetzel, 1992; Wetzel, 2001). The opposite occurs if the river is oversaturated with respect to CO_2 ($pCO_{2\ water} > pCO_{2\ atmosphere}$). The latter process of CO_2 evasion is still poorly quantified. Estimations of global average evasion fluxes from rivers changed from early values in the range of ~0.01 Pg C yr^{-1} (Kempe, 1982) to still diverse values of 0.35 Pg C yr^{-1} (Cole et al., 2007), 1.8 Pg C yr^{-1} (Raymond et al., 2013) and 0.65 Pg C yr^{-1} (Lauerwald et al., 2015). Specifically the contribution of small headwater catchments seems to be an important but so far not well-explored factor (Butman and Raymond, 2011; Cole et al., 2007; Duvert et al., 2018; Halbedel and Koschorreck, 2013; Johnson et al., 2008; Marx et al., 2017).

Since CO_2 is responsible for a major part of the greenhouse effect and global climate change (IPCC, 2014), a sound knowledge of the riverine carbon cycle is important as input parameters for climate models, to predict future temperature and precipitation evolution.

Aside from CO_2 evasion, evaluating the origin of TCO_2 in rivers can help to understand the interaction of different water compartments (for instance the importance of groundwater contribution to the river) or the importance of weathering processes and water–rock interaction in the catchment (Doctor et al., 2008). Therefore, assessment of riverine TCO_2 provides a necessary base of knowledge for future decisions on the sustainable management of water resources.

A powerful tool for investigating the TCO_2 system is the stable carbon isotope ratio ($^{13}C/^{12}C$), denoted as $\delta^{13}C$. Together with the pCO_2 and the concentration of TCO_2 (TCO_2), $\delta^{13}C$ values are used to differentiate between above-mentioned processes.

Recent studies showed that CO_2 evasion from streams and small rivers play a significant role in the carbon system (Raymond et al., 2013; Ward et al., 2017). This is especially true for headwater streams with no or only limited hydro-chemical data available (Marx et al., 2017). While rivers in karst dominated catchments were identified as highly CO_2 supersaturated (Lee et al., 2017; van Geldern et al., 2015) with maximum values up to 55 times higher than the current atmospheric level at a temperate perennial karst spring (van Geldern et al., 2015), the situation is expected to be completely different in high-altitude catchments with granitic or metamorphic lithologies, where carbon sources from carbonate weathering and soil CO_2 from vegetation are largely missing.

As a pilot study site with high elevation and contrary geology to karst, we selected the island of Corsica in the western Mediterranean with its steep topographic gradient (i.e. high relief) and its diverse, but largely granitic and metamorphic lithology. This study was conducted along the Tavignanu River in eastern central Corsica (Fig. 1), a river with a high morphological gradient that flows through three different lithologies. The major objective of the study was to identify and quantify influences on freshwater CO_2 degassing such as different lithology (granitic, metamorphic, and coastal sedimentary plain sediments) and variable land use along a river course with a steep altitudinal gradient.

2. Study area

The Tavignanu River and its tributaries are located in the eastern part of the island of Corsica, France (Fig. 1). On a total length of 89.1 km the main river descends from 1875 m.a.s.l. to sea level. With respect to morphology, the Tavignanu River can be divided into three sections: (1) The uppermost part from the source to the city of Corte flows ENE for about 27 km and quickly drops about 1475 m of height in a high mountain environment. (2) Downstream from Corte, the river changes direction to roughly SE and cuts the lower mountain range of the Castagniccia region on a stretch of 40 km. (3) For the last 22 km, the river enters the low gradient coastal region and eventually discharges near the city of Aléria into the Tyrrhenian Sea.

With a N-S-extent of 30 km and an E-W-extent of 53 km, the entire catchment of the Tavignanu River including its tributaries spans an area of 799 km^2 (Fig. 2). The highest mountain in the catchment is the Monte Rotondo that peaks at 2622 m.a.s.l. Four geologic compartments compose the drained area. In the West, the crystalline Corsica forms the high mountain range consisting of plutonic basement rocks, which are mainly granites uplifted by the Variscan orogeny (Rossi and Cocherie, 1991). Different, partly metamorphosed, sedimentary rocks, such as limestones and sandstones from the Triassic to Eocene, follow to the East in the central depression (Caron and Bonin, 1980). The adjoining schistose or alpine Corsica accounts for the low mountain range in the Castagniccia region with ophiolites and former ocean sediments metamorphosed to schist and other metamorphic rocks (Egal, 1992). Adjacent to the sea, the coastal plain, called *Plaine Orientale*, is composed of post-glacial alluvial and marine sedimentary rocks (Orszag-Sperber and Pilot, 2013). It is widely used for agricultural cultivation of grapevine, citrus fruits, and olives.

Corsica is characterized by a Mediterranean climate. The mean annual temperature and precipitation for Corte, in the middle of the catchment, are 14.1 °C and 820 mm. Due to the high relief, mean temperatures and precipitation vary considerably with altitude. Long-term temperature and precipitation averages of three selected locations in the catchment are shown in Table 1. Additionally, temperature, precipitation, and discharge time series from January 2016 to April 2017 of the Tavignanu are presented in Fig. 3.

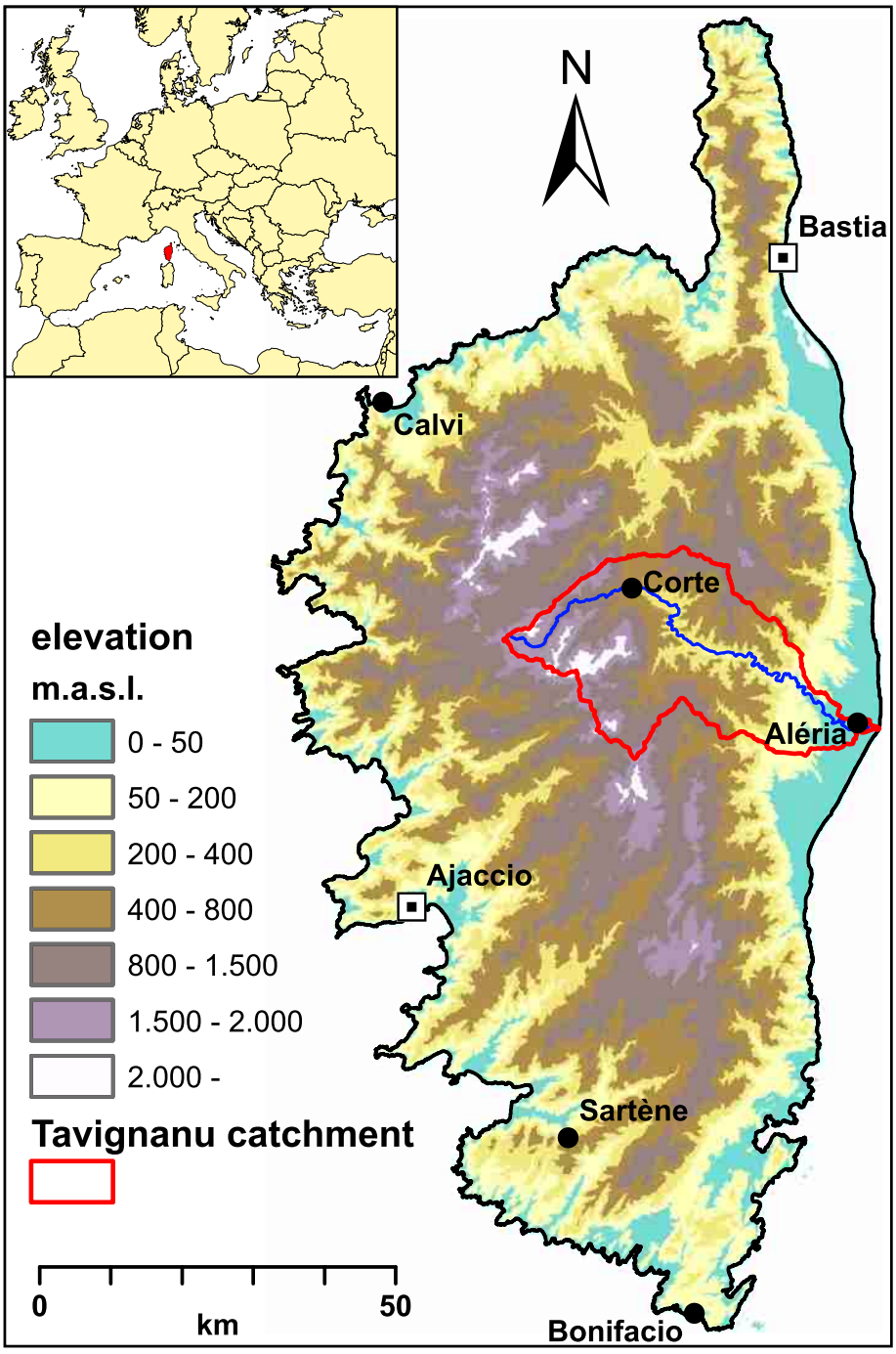

Fig. 1. Topographic map of the island of Corsica (France) with the location of the Tavignanu River (blue) and borders of its catchment (red).

3. Methods

3.1. Sampling sites

Ten sampling points were set along the Tavignanu River, the main receiving stream (sampling points 1 to 10 in Fig. 2). Additionally, water from six major tributaries was sampled at eleven points (named R1 to R6 and I to V). A list of all sampling points with their location is provided in Table 2. Tributary sample points were chosen near their respective mouths to receive a representative sample of the entire subwatershed. The Tavignanu River sampling sites were set after the inflows of the tributaries, to attain a homogenous mixture of both water masses. This is necessary, to recognize and potentially quantify influences of the tributaries. Downstream of Corte, this resulted in an almost evenly distributed pattern along the Tavignanu River (Fig. 2). A special focus was put on the Restonica River, which is the first, larger water contributor to the main channel. In contrast to the upper Tavignanu valley, west of Corte, the Restonica valley is for the most part, easily accessible by car. Since the remoteness of the western Tavignanu River prohibited a regular sampling point distribution, the Restonica River was selected as a comparable substitute. The roughly similar river course with respect to height, length and lithology justifies that approximation and finally six sampling points were established along the Restonica River (R1 to R6).

Both, Tavignanu and Restonica rise from source lakes, namely Lac de Ninu and Lac de Melu, respectively. The lakes serve as pools that collect

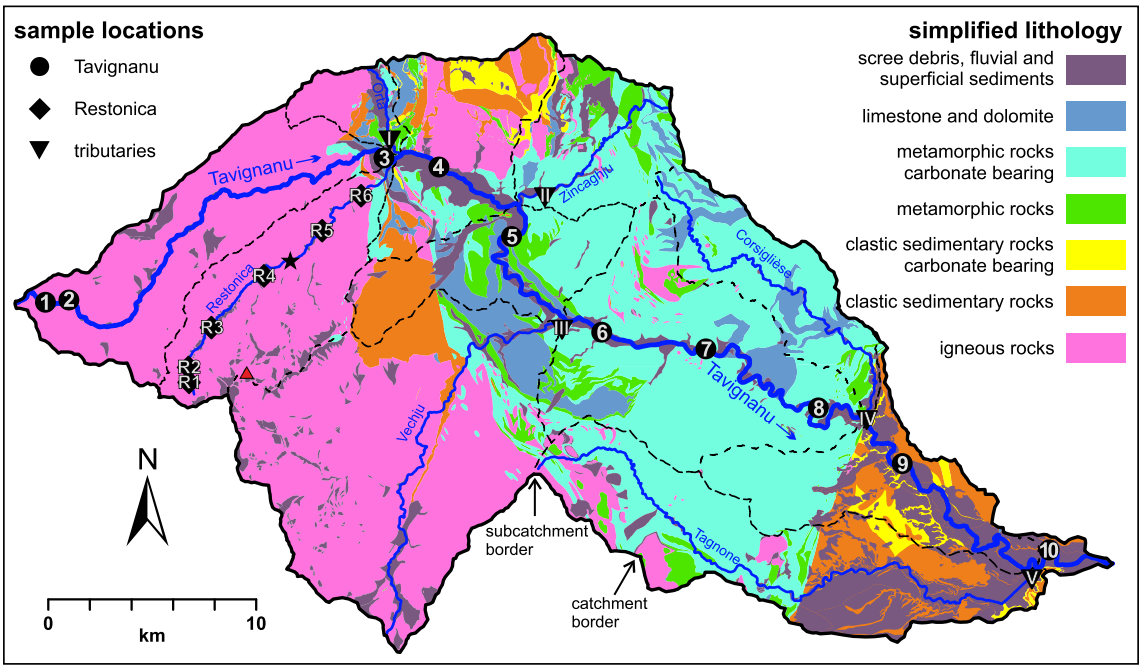

Fig. 2. Simplified geologic map (Map basis: BRGM) of the Tavignanu River catchment (area: 799 km^2). Sampling points are shown for the Tavignanu River (circles), the Restonica River (diamonds) and other major tributaries (triangles). Gauging stations in the catchment exist for the Restonica River, the Vechju River (stars), and the Tavignanu River (at sampling point 8). The highest peak in the catchment (Monte Rotondo, 2622 m.a.s.l.) is shown as reference (red triangle). For a list of the sampling locations and their upstream distances refer to Table 2.

the precipitation on the surrounding mountainsides. The respective first sampling point was placed directly at the outflow of the lakes. Sampling took place in 2016 on a quarterly basis with each campaign representing winter (February), spring (May), summer (July), and autumn (October).

3.2. Field parameters and sampling

Every sample point was examined for the in situ physico-chemical field parameters water temperature (T), pH value, electrical conductivity (EC), and total alkalinity (TA). Total alkalinity was analyzed by titration using a Hach Digital Titrator (Model 16,900, Hach Company, Loveland, CO, U.S.A.). Based on the results of ion analysis, we assumed absence of significant amounts of alternate TA contributing species, e.g. $H_3SiO_4^-$ (Wolf-Gladrow et al., 2007). Therefore, carbonic species represent the sole buffer in this system. The TA value determined by acid titration then directly corresponds to carbonic alkalinity. Titration was performed on 100 mL samples until the titration endpoint was indicated by a colour change from indicators bromcresol green to methyl red. Based on repeated analysis, the precision of the manual titration is about ±5 instrument digits, resulting in an analytical precision of either ±0.5 mg L^{-1} or ± 5 mg L^{-1} $CaCO_3$ when using sulfuric acid with equivalent concentrations of 0.16 eq. L^{-1} or 1.6 eq. L^{-1}, respectively. Physico-chemical field parameters were measured with a multi-parameter instrument WTW Multi 350i (WTW GmbH, Weilheim, Germany). Instrument precision (±1σ) is about 0.1 °C for temperature, 0.05 for pH, and 2% for EC. Measured EC values were automatically normalized to 25 °C based on the non-linear temperature compensation function for natural waters.

All water samples were taken mid-stream wherever possible and filtered through 0.45 μm syringe disk filters (Minisart HighFlow PES, Sartorius AG, Germany). Samples for major ions were filled in two 50 mL HDPE bottles (Gosselin, Hazebrouck, France). Trace metal samples were sampled into 15 mL polypropylene conical centrifuge tubes (Falcon tubes, BD Biosciences, Bedford, USA). Additional samples were taken for the concentration (TCO_2) and stable isotope analysis of dissolved inorganic carbon ($\delta^{13}C_{DIC}$) in 40 mL amber borosilicate glass vials that fulfill the specifications of the US Environmental Protection Agency (so-called EPA vials). The open-hole caps of the EPA vials were equipped with flipped butyl rubber-PTFE septa, the butyl rubber side facing inside, to improve gas tightness. Beforehand, the EPA vials were poisoned with a few drops of nearly saturated $HgCl_2$ solution (~50 g L^{-1}), to prevent any microbial alteration of the carbon species during sample storage. EPA vials were filled to maximum capacity and capped without air bubbles. All of the above described sample containers were tightly sealed with Parafilm® and stored cool (~4 °C) and dark.

Table 1
Average climate data for three selected sites for the interval 2000–2015 (Météo-France). Corte values are measured; high mountain and coast values are from modeled datasets (SIM-France, Météo-France).

	High mountains (near source lakes)	Corte	Coast (near Aléria)
Elevation/m.a.s.l.	~1500–2500	~400	~0
Average temperature in January/°C	−0.1	6.2	9.1
Average temperature in July/°C	15.5	23.0	25.1
Mean annual temperature/°C	6.8	14.1	16.4
Mean annual precipitation/mm	1390	820	830

3.3. Laboratory analyses

3.3.1. Stable carbon isotopes

Stable isotopes of DIC were determined via continuous flow isotope ratio mass spectrometry (CF-IRMS) on a Delta *plus* XP coupled to an automatic equilibration unit GasBench II (Thermo Fisher Scientific Inc., Bremen, Germany). For analysis water was transferred from the closed 40 mL EPA vials into helium flushed (gas purity 99.999%) 12 mL Exetainer® vials (Labco Limited, Lampeter, Wales, UK) via disposable syringes. An argon-filled sampling bag (Grace, Deerfield, IL, USA) was connected to the EPA vial through a second needle to allow the extracted water volume to be replaced by inert gas and thus preventing headspace contamination by atmospheric CO_2. During injection into the Exetainer, its septum was punctured by yet another cannula to

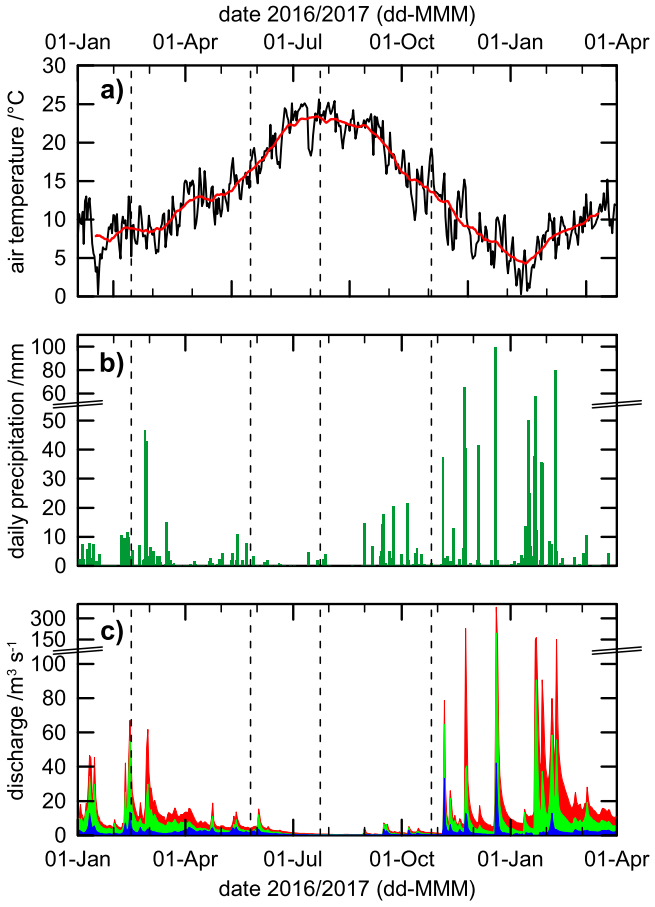

Fig. 3. Air temperature, rainfall (from station 20096008 Corte Aérodrome, Météo-France), and discharge data (HYDRO - MEDDE/DE) from January 2016 to April 2017. Red line in the temperature plot is the 31-day running average. Discharge is presented for Tavignanu River (red), Vechju River (green), and Restonica River (blue). The respective locations are shown in Fig. 2. Dashed lines indicate dates of sampling. Note that discharge and precipitation plots have broken *y*-axes, which indicate a change of scale.

Table 2
List of sampling sites with coordinates (in coordinate system WGS 1984), elevation in meters above sea level (m.a.s.l.), and downstream distance to the mouth of the Tavignanu River. Note that distance values for "Other tributaries" mean the distance between the respective tributary mouth and Tavignanu River mouth.

Site ID	Latitude	Longitude	Elevation	Distance from mouth
	°N	°E	m.a.s.l.	km
Tavignanu River				
1	42.25348	8.94436	1745	87.2
2	42.25371	8.95795	1735	85.8
3	42.30444	9.14704	419	63.2
4	42.29867	9.17839	357	60.1
5	42.26622	9.21720	265	53.2
6	42.22204	9.26521	178	43.2
7	42.21131	9.32486	134	37.6
8	42.18183	9.38659	73	27.3
9	42.15517	9.43290	17	18.1
10	42.11245	9.51384	1	4.0
Restonica River				
R1	42.21417	9.02353	1710	79.7
R2	42.22069	9.02392	1525	78.9
R3	42.23687	9.03939	1266	76.5
R4	42.25772	9.07164	931	72.6
R5	42.27542	9.10732	638	68.4
R6	42.28896	9.13176	471	65.3
Other tributaries				
I - Orta	42.31328	9.15144	390	62.2
II - Zincaghju	42.28440	9.23870	289	55.3
III - Vechju	42.22752	9.24279	191	45.2
IV - Corsiglièse	42.17807	9.41594	29	22.1
V - Tagnone	42.10267	9.50319	3	5.1

restrain headspace pressure by allowing the sample to displace helium gas. Sample TCO_2 was converted to CO_2 by adding small amounts of 85% H_3PO_4 after cannula removal by a syringe through the vial's septa. The transferred water volume was chosen to attain a detector signal height between ~4.0 and ~7.5 V (*m*/*z* 44) for the isotope ratio mass spectrometer (van Geldern et al., 2015). The necessary volume depended on the expected TCO_2 content, which was estimated from TA values, and ranged from 0.5 to 6 mL. Samples were analyzed in duplicates and the reported value is the mean value. Conventionally, the delta notation for the relative difference of isotope ratios is used for isotope values and is denoted in per mil (‰):

$$\delta^{i}\mathrm{E} = \frac{R\left({}^{i}\mathrm{E}/{}^{j}\mathrm{E}\right)_{\mathrm{sample}}}{R\left({}^{i}\mathrm{E}/{}^{j}\mathrm{E}\right)_{\mathrm{reference}}} - 1 \quad (1)$$

R represents the ratio of heavy isotopes (mass *i*) to light isotopes (mass *j*) of an element E for a sample or a reference substance (Coplen, 2011). Attained data was corrected for instrumental drift and normalized to the Vienna Pee Dee Belemnite (VPDB) scale by assigning a value of +1.95‰ and −46.6‰ to the reference materials NBS 19 and LSVEC, respectively (Brand et al., 2014). Accuracy and external reproducibility is based on the repeated analyses of a carbonate control sample and was better than 0.1‰ (±1σ) for $\delta^{13}C_{DIC}$.

Concentration of total dissolved inorganic carbon (TCO_2) was determined from the peak areas of the chromatogram of the isotope ratio measurement. Areas of sample peaks are directly proportional to the amount of CO_2 liberated by the reaction of the sample with phosphoric acid. A set of standards with known TCO_2 concentrations was prepared by dissolving $NaHCO_3$ in TCO_2-free, ultrapure water (Milli-Q Integral, EMD Millipore Corporation, Billerica, MA, USA). This calibration set was included in every run. Peak areas were adjusted for the exact individual sample volume. The exact amount of water in each vial was determined by weighing. For conversion to volume, a sample density of 1.0 g cm^{-3} was assumed. Concentration of TCO_2 is reported in milli mol per liter (mmol L^{-1}). Accuracy of analyses was monitored by repeated analysis of a standard with known concentration during the run. Precision (i.e. reproducibility) was better than 0.05 mmol L^{-1} (± 1σ).

3.3.2. Calculation of pCO_2

TCO_2 consists of different species, whose distribution can be determined from water temperature, pH, and TCO_2 values by using chemical equilibrium equations and constants (e.g. Deines et al., 1974; Plummer and Busenberg, 1982). pCO_2 is then related to the CO_2 concentration in the sample and can be calculated using Henry's law constant. The final combined equation solved for pCO_2 is

$$pCO_2 = \frac{TCO_2}{K_H \cdot \left(1 + \frac{K_1}{H^+} + \frac{K_1 \cdot K_2}{(H^+)^2}\right)} \quad (2)$$

where K_H is the Henry's law constant, K_1 and K_2 are the equilibrium constants for the first and second deprotonation reaction of dissolved CO_2, and H^+ is the concentration of protons calculated from pH. The temperature dependence of equilibrium constants is expressed in empiric equations taken from Plummer and Busenberg (1982). For equilibrium constants and Eq. (2) standard deviation was calculated based on error

propagation with the assumption of measurement precisions of 0.05 for pH, 0.05 mmol L^{-1} for TCO_2, and 0.1 °C for temperature.

3.3.3. Air-water flux of CO_2

The amount of CO_2 that diffuses from water to air can be calculated by the following equation (Raymond et al., 2012)

$$F_{CO_2} = k\cdot([CO_2]_{water} - [CO_2]_{air}) \quad (3)$$

where F_{CO_2} is the CO_2 flux from water to atmosphere, k is the gas transfer velocity, and $[CO_2]$ are the respective molar CO_2 concentrations. Values of k are often normalized to a Schmidt number of 600 and then denoted as k_{600}, which corresponds to CO_2 in freshwater at 20 °C. Raymond et al. (2012) presents a compilation of different equations for the calculation of k_{600}. A further comparison of these equations was done by (Maurice et al., 2017). The best performing formula was Model equation 5 from Table 2 of (Raymond et al., 2012), which was consequently used in this study:

$$k_{600} = V\cdot S\cdot 2841 + 2.02 \quad (4)$$

with V as the stream velocity and S as the slope of the riverbed. V was calculated from average discharge values for each month and the cross-sectional area of the main channel. The slope S was taken from a topographic transect along the river. For the estimation of V and S, the Tavignanu River was separated into two sections: the steeper, fast flowing upper Tavignanu valley and the section downstream of Corte that is the lower more gently declining part. The calculated values of k_{600} are given in results section (Table 3).

3.3.4. Selection of endmember values

Since different sources of carbon contribute to the riverine pool of TCO_2, constraining values for these endmembers have to be assumed. Based on measurements on the Mediterranean island of Lampedusa in late 2015, the partial pressure ($pCO_{2\ atm}$) and the isotopic composition of atmospheric CO_2 ($\delta^{13}C_{CO_2\ atm}$) are assumed to be 403 µatm and −8.5‰ VPDB for the study period (ESRL/GMD, 2016). Soil CO_2 exhibits isotope values derived from the photosynthetic pathway of the plant it is derived from (~−27‰ for C3 plants, Ehleringer and Cerling, 2002) and fractionation influence from diffusive outward degassing, which in turn depends on soil pCO_2. With the adoption of average soil pCO_2 values from Mediterranean climate (Piñol et al., 1995) for this study, $\delta^{13}C_{CO_2\ soil}$ values between −19.0 and −21.8‰ can be assumed. During slow groundwater discharge to springs or gaining streams, weathering of rock via dissolution of minerals, like carbonates and silicates, further modifies amount and carbon isotope ratio of TCO_2. Carbonate weathering produces a stoichiometric 1:1 mixture of CO_2 and dissolved carbonate. A catchment average for carbonate $\delta^{13}C_{CaCO_3}$ was extracted from supplementary data of Cartwright and Buick (2000) and own samples, and equals (−0.6 ± 1.4) ‰ VPDB (n = 14). With the above mentioned values for $\delta^{13}C_{CO_2\ soil}$ a 1:1 mixture is then expected around −10‰. Silicate weathering introduces no new carbon to the system, but shifts carbon species equilibrium and can result in similar isotope values. Due to the much higher dissolution rates of carbonates compared to silicates (e.g. calcite: ~10^{-5} mol m^{-2} s^{-1}; K-feldspar: ~10^{-17}–10^{-12} mol m^{-2} s^{-1}) (Chamberlain et al., 2005), even in silicate dominated terrain, trace carbonates can contribute noticeably to TCO_2 (Leybourne and Goodfellow, 2010), especially if TCO_2 is low.

Table 3
Seasonal values for the gas transfer velocity k_{600} (calculated after Eq. (4), median values for pCO_2 (calculated from T, pH, and TCO_2, after Eq. (2)), and F_{CO_2} (calculated after Eq. (3). Positive values of F_{CO_2} indicate degassing of CO_2, negative values indicate CO_2 dissolution in water.

	k_{600} (upper Tavignanu)	k_{600} (lower Tavignanu)	Median pCO_2[a]	Median F_{CO_2}
	m d^{-1}	m d^{-1}	µatm	mmol m^{-2} d^{-1}
February	25.9 ± 13.8	5.5 ± 1.9	167	−34.9
May	26.9 ± 12.6	6.1 ± 1.8	353	−0.7
July	13.8 ± 7.3	2.9 ± 0.5	579	+8.9
October	20.9 ± 13.0	4.3 ± 1.5	527	+33.5

[a] Atmospheric value for comparison: 403 µatm.

4. Results

Downstream transects of various parameters are shown in Fig. 4. Detailed analytical results are available as online supplementary material

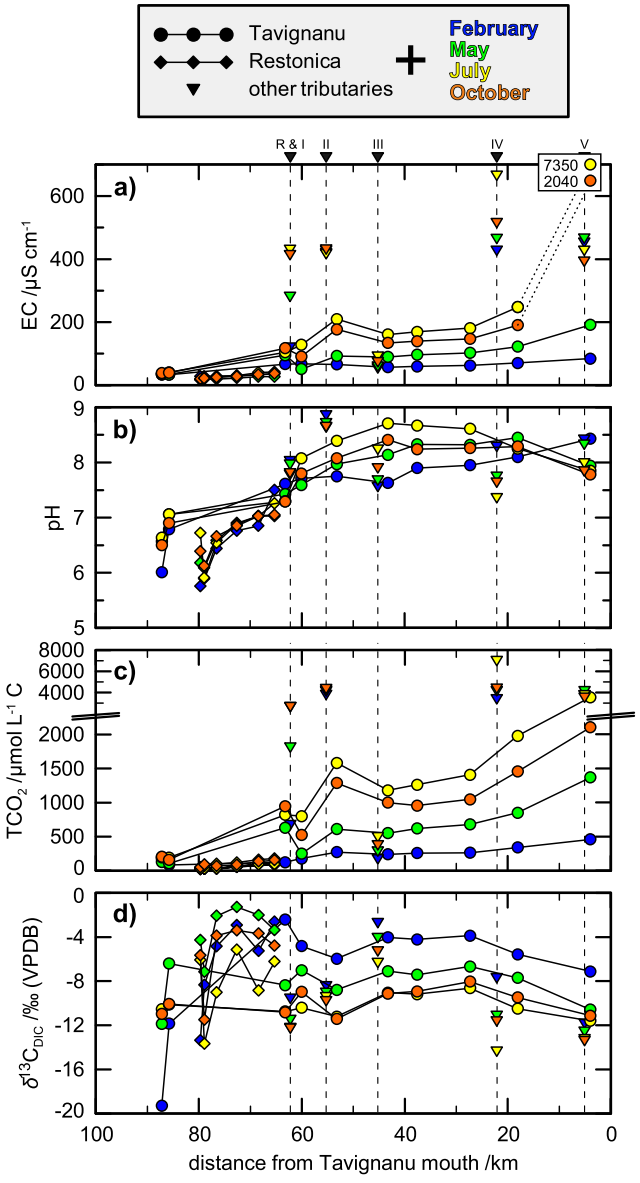

Fig. 4. Results of a) EC, b) pH, c) TCO_2, and d) $\delta^{13}C_{DIC}$ plotted against downstream distance of the respective sampling point. Different rivers are symbol coded; months are colour coded. Dashed vertical lines indicate confluences with tributaries. Axes break for TCO_2 indicates a change of scale. Errors of ±1σ are within symbol size.

from the journal's website and are additionally archived in the World Data Center PANGAEA[1] for long-term storage and free access.

4.1. Electrical conductivity and pH

Electrical conductivity (Fig. 4a) remained stable at the Lac de Ninu with (36 ± 2) µS cm^{-1} (±1σ). Both, spatially and seasonally, EC values showed a general increase with downstream distance and approaching summer months. In February the Tavignanu River remained stable between sampling point 3 and 9 with an average value of (64 ± 5) µS cm^{-1}. Sampling point 10 showed a discernible increase to 84 µS cm^{-1}. In May, July, and October the overall downstream trend steepened, with an exceeding increase between the samples of point 9 and 10. Outliers of this evolution include sample 4 of May, where the Restonica River and the Orta River (I) have entered the main stream, and sample 5 of July and October after the confluence with the Zincaghju River (II). For the most sections, values were below 250 µS cm^{-1}, with the exception of the lowermost sampling points in July and October with values beyond 2000 µS cm^{-1}. The Restonica River showed minimal spatial and seasonal variation. A uniform increase from Lac de Melu to sampling point R6 was observed, with values from 28 to 37 µS cm^{-1} in February, 18 to 27 µS cm^{-1} in May, 17 to 42 µS cm^{-1} in July, and 20 to 36 µS cm^{-1} in October.

Distribution of pH values along the Tavignanu River and the Restonica River (Fig. 4b) was highly variable between the observed minimum and maximum values of 5.8 and 8.7 pH units. In February, pH increased steadily over the entire downstream distance from 6.0 to 8.4, with a slight depression at sample 6. During May and July, the pH maximum moved upstream to sample 9 with 8.5 and sample 6 with 8.7, respectively. October values were similar to May. At large, higher values could be detected in summer. Temporal pH change at the source lake and sample 2 happened from February (6.0 and 6.8, respectively) to May (6.6 and 7.1), with no further difference to July (6.6 and 7.1) and a minor decrease in October (6.5 to 6.9). In general, the steepest spatial pH increase occurred between Lac de Ninu and sampling point 2. The Restonica River presented a temporally uniform increase from source lake to mouth. Only Lac de Melu itself varied strongly, with a seasonal increase to summer. The pH value progress to sample R2 was positive in February (5.8 to 5.9), slightly negative in May (6.2 to 6.1), strongly negative in July (6.7 to 5.9), and moderately negative in October (6.4 to 6.1).

4.2. TCO_2 and stable isotope values

In the Tavignanu River, the total content of dissolved inorganic carbon (TCO_2) (Fig. 4c) exhibited seasonal differences and a spatial evolution similar to the EC values. The source value at sampling point 1 changed from 173 µmol L^{-1} in February to 128 µmol L^{-1} in May, reached 195 µmol L^{-1} in July, and climbed to a seasonal maximum at this point of 205 µmol L^{-1} in October. Near the Tavignanu River mouth (sampling point 10), values also showed a seasonal cycle with 460, 1370, 3567, and 2105 µmol L^{-1} in February, May, July, and October, respectively. The downstream trend in February appeared uniform with an increase of about 4 µmol km^{-1}. In May, July, and October, the trend became more diverse. The Restonica source lake features very low TCO_2 values with 41, 24, 22, and 52 µmol L^{-1} in February, May, July, and October. Overall, the Restonica downstream course exhibited an increase to a maximum value of 179 µmol L^{-1} at sample point R6 in July.

Values of total alkalinity (TA) in the Tavignanu and Restonica River mainly followed the trends of TCO_2 and EC values. With 48, 128, 174, and 170 µmol L^{-1}, in February, May, July, and October, seasonal differences at the Tavignanu source lake were small. The highest TA values, in the Tavignanu River, of each month was observed at the sampling point closest to the river mouth, with 511, 1259, 2697, and 1878 µmol L^{-1}, in February, May, July, and October.

Carbon isotope values of dissolved inorganic carbon ($\delta^{13}C_{DIC}$) in the Tavignanu River varied spatially and seasonally between −19.3‰ and −2.4‰, with most variation between the first three sampling points (Fig. 4d). The observed $\delta^{13}C_{DIC}$ difference between sample 1 and 2 was most prominent in February with +7.4‰, lower in May (+5.5‰) and small in July (+0.4‰) and October (+0.9‰). In February, $\delta^{13}C_{DIC}$ values further increased to sampling point 3. Downstream of sampling point 3, the overall pattern of $\delta^{13}C_{DIC}$ values was similar, independent of the season. Values in July and October were almost identical and at the annual minimum. May and February exhibited an average positive shift of (2.2 ± 0.8) ‰ between May and July, and (2.8 ± 0.5) ‰ between February and May. The Restonica River differed from the Tavignanu main stream both seasonally and spatially. In February, values increased from source to mouth, with the exception of sample R5. May, July, and October exhibited an initial decrease between R1 and R2, but values increased again downstream.

4.3. pCO_2 and F_{CO_2}

The calculated pCO_2 values for water samples express theoretical equilibrium conditions (Fig. 5) and were calculated from *T*, pH, and TCO_2. In the case of the Tavignanu River, seasonal variations were strongest at the upper course before Corte and at the two lowermost sampling points in summer.

At the Tavignanu source lake outflow (sample 1), pCO_2 values changed from 1814 in February, over 1180 in May, to 1708 in July, and back to 1846 µatm in October. At these locations the water was supersaturated compared to the atmospheric pCO_2 value of ~403 µatm, which is the average value for late 2015, measured on the

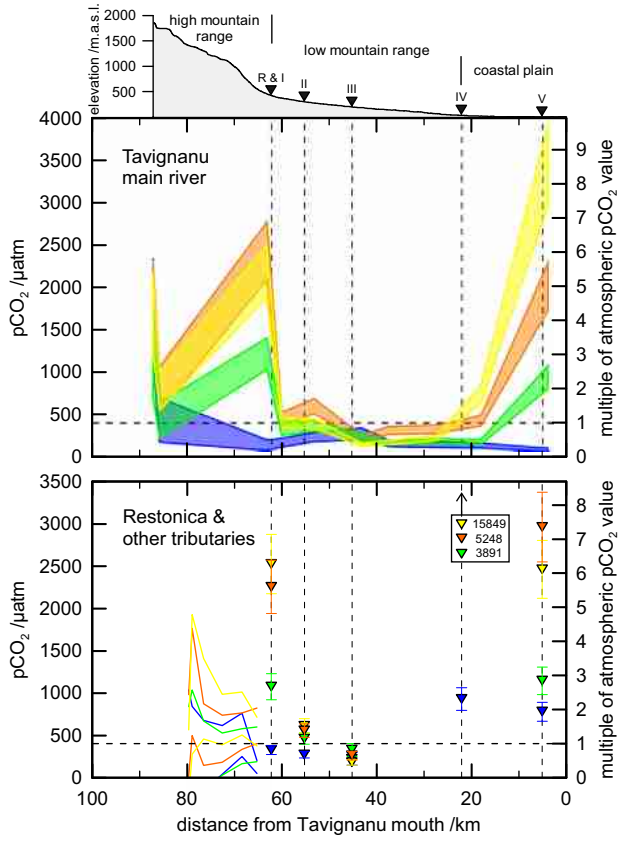

Fig. 5. Downstream transect of calculated values for pCO_2. Dashed horizontal line represents atmospheric concentration of CO_2. Right hand axis shows CO_2 concentrations as multiple of atmospheric value. For symbol legend see Fig. 4.

[1] www.pangaea.de, DOI: https://doi.org/10.1594/PANGAEA.896606

Mediterranean island of Lampedusa (ESRL/GMD, 2016). Sample 2 is around atmospheric pCO_2 levels in February and May, and around twice the atmospheric level in July and October. After the general steep decline between samples 1 and 2, sample 3 of February continued the declining trend and reached undersaturation with respect to atmospheric pCO_2 levels. During the other seasons, values at the end of the upper Tavignanu valley show higher CO_2 concentrations compared with the vicinity of the source lake. The downstream course after point 3 mainly remained undersaturated, with a minimum value of 88 μatm at point 10 in February. Sampling points closer to the river mouth showed a pCO_2 increase to supersaturation after springtime, with a maximum of 3427 μatm for the Tavignanu River in July.

In February and May, the Restonica River was almost completely undersaturated. In July and October an increase up to the second sampling point was followed by a gradual decline of pCO_2 values to near atmospheric levels.

Seasonal averages of pCO_2, F_{CO_2}, and the gas transfer velocities k_{600} used for their calculation are collected in Table 3. Since pCO_2 and F_{CO_2} exhibited a strongly skewed distribution in the downstream transect, the more robust median was used as the better indicator of central tendency.

5. Discussion

5.1. Seasonal and spatial variations of field parameters

Electrical conductivity shows low and stable values at the source area (Fig. 4a). This suggests that no significant weathering happens around the source lakes, which would increase EC values and induce a seasonal pattern. In February most of the EC increase happens until sampling point 3. Downstream of Corte further changes are almost indiscernible. In May, the same pattern with slightly higher EC values could be observed. Additionally, the influence of tributaries on conductivity was detectable, especially at the confluence with the Restonica River. In July and October, the mixing of water masses at tributary inflows was even more pronounced in EC values. Altogether, the observed seasonality with increased EC values during warmer months indicates chemical weathering, which is enhanced by higher temperature, lower discharge, and increased availability of corroding agents, such as CO_2. Slight increases between sampling points 6 and 8 in May to October can be attributed to evaporation. The steep increase towards sampling point 10 in July and October can also be found in the concentrations of several ions, such as Na^+ and Cl^-. It can be the result of groundwater flow through former salt marshes, that were drained to be used as pastures. Additionally, sea water could possibly intrude from the lagoon *Étang de Diane* in the near vicinity, when the discharge of the river is low in summer.

5.2. Main stream TCO_2 dynamics

5.2.1. Upper silicate catchment of the Tavignanu and Restonica River

In the case of the Tavignanu River, spatial as well as seasonal influences on the carbon system exist. Near the source areas, TCO_2 and TA exhibited low values compared with the downstream trend, during all months. This means the buffer capacity is also low, and even a slight addition of carbon species results in prompt pH changes. The same is true for $\delta^{13}C_{DIC}$ values, which can be changed considerably by exchange of minor quantities of carbon. This is expressed in the initial CO_2 degassing between sample 1 and 2, where in February, the rapid drop of pCO_2 is accompanied by a steep increase of $\delta^{13}C_{DIC}$ and pH. In May, July, and October, a similar decrease of pCO_2 results in less pH and $\delta^{13}C$ change. This is due to higher buffering of the slightly higher TCO_2 and pH, which is derived from enhanced weathering during the warmer months.

The evolution from sample 2 to 3 exhibits the most pronounced seasonal changes. In winter, pCO_2 drops well below atmospheric levels and $\delta^{13}C_{DIC}$ values increases from −11.9 to −2.4‰, although TCO_2 does not increase extensively. During May, July, and October, pCO_2 and TCO_2 increase noticeably, and $\delta^{13}C_{DIC}$ shows little spatial evolution. The increase of TA in winter can be explained by a combination of silicate and trace carbonate weathering. This consumes more CO_2, than can be replenished by the atmosphere. Since the minor amount of dissolved carbonate cannot account for the strong increase in $\delta^{13}C_{DIC}$, an additional process has to be considered. When pCO_2 in water has reached values near atmospheric composition, isotopic exchange with the atmospheric CO_2 can occur (Doctor et al., 2008). The equilibrium fractionation between gaseous CO_2 (here $\delta^{13}C_{CO_2\ atm} = -8.5‰$) and TCO_2 depends on the temperature and species distribution, i.e. T and pH. In the case of sample 3 in February, atmospheric equilibrium $\delta^{13}C_{DIC}$ would be +0.9‰ (Clark and Fritz, 1997). The measured value of −2.4‰ does indicate a not completely reached equilibrium with the atmosphere. This is either because of influence by an additional CO_2 source, e.g., from in-river processes such as respiration or decay, or because of incomplete isotopic exchange with the atmosphere. Isotopic equilibration between rivers and the atmosphere can take several weeks to establish (Aucour et al., 1999; Cartwright, 2010), thus making the latter process more likely.

In spring, summer, and autumn, the evolution between sample 2 and 3 shows an increase in pCO_2, TCO_2, and TA, accompanied by a relative stable $\delta^{13}C_{DIC}$ value. Higher productivity of plants in spring and summer results in increased organic matter and respiration in soils (Barth and Veizer, 1999; Hope et al., 2004; Shin et al., 2011). Together with the longer residence time of water in soils, due to low precipitation, higher CO_2 content in soils can cause stronger weathering of both silicates and trace carbonates and result in elevated pCO_2, TCO_2, and TA. In the case of carbonate weathering, open system conditions for soils can be assumed, because the granitic lithology in the upper Tavignanu and Restonica catchment does not allow for the development of thick soil zones. During silicate weathering, no difference occurs between open and closed system for $\delta^{13}C_{DIC}$. The possible contribution of carbonate to $\delta^{13}C_{DIC}$ can then be ignored, and only dissolution of soil CO_2 determines the $\delta^{13}C_{DIC}$ value. The equilibrium fractionation during CO_2 dissolution is about 10‰ (e.g., Mook et al., 1974). The measured values of −8.4‰, −10.7‰, and −10.8‰ for May, July, and October, respectively, can thus be interpreted as the result of dissolved $\delta^{13}C_{CO_2\ soil}$ values of ~−18‰ and −20‰, respectively. The small differences between May, July, and October are due to increased pCO_2 in soils at warmer temperatures, which influences $\delta^{13}C_{CO_2\ soil}$ by diffusive degassing to the atmosphere (Davidson, 1995). Low solubility of silicates prevents the consumption of all generated soil CO_2.

The Restonica River experiences roughly the same trend, but on a smaller scale. As mentioned above, the source lake is influenced by photosynthesis in summer. From sampling point R1 to R2, the Restonica River gains noticeable amounts of water through small runlets. Thus, sample R2 is regarded as more representative for ground/soil water conditions. In February, May, and October minor weathering produces small values of TCO_2, TA, and pCO_2. Since pCO_2 is near atmospheric values, isotopic exchange with atmosphere is possible and high values of $\delta^{13}C_{DIC}$ occur. In July, where CO_2 content in soils is higher, weathering is enhanced, like in the upper Tavignanu valley. Hence, riverine $\delta^{13}C_{DIC}$ values were lower and in the range of $\delta^{13}C_{CO_2\ soil}$ values after dissolution.

5.2.2. Comparison of tributaries and their seasonal variations

Seasonal evolution has the same tendency for almost every tributary. From winter to summer, TCO_2, TA, and pCO_2 increase, while pH and $\delta^{13}C_{DIC}$ decrease. Tributary classification can be done with focus on TCO_2 and $\delta^{13}C_{DIC}$ (Fig. 6). Tavignanu, Restonica, and Vechju River (III) generally have low TCO_2 values and a large variety of $\delta^{13}C_{DIC}$ values. They exhibit strong seasonal changes in carbon $\delta^{13}C_{DIC}$ values, but small variations in inorganic carbon content. These rivers are dominated by their mainly silicate catchment, which allows for isotopic evolution via

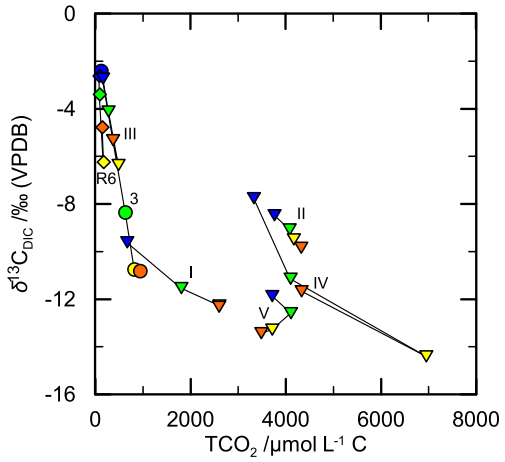

Fig. 6. Seasonal evolution of carbon content (TCO_2) and carbon isotope ratios ($\delta^{13}C_{DIC}$) of tributaries. The Tavignanu River is plotted with its last sampling point before the confluence with Restonica River. For symbol legend see Fig. 4. Errors of $\pm 1\sigma$ are within symbol size.

increased soil CO_2 input, but limits TCO_2 increase, due to missing carbonate sources. Instead, the excessive CO_2 enhances silicate weathering.

The Orta River (I) shows intermediate carbon concentrations and seasonal changes in $\delta^{13}C_{DIC}$ values and TCO_2 evolution. Carbonate rocks in its catchment are subject to increased weathering in summer, which elevates TCO_2. The observed $\delta^{13}C_{DIC}$ decrease to −12.3‰ indicates that carbonate dissolution occurs under open system conditions. The same seasonal evolution is present in the Corsiglièse River (IV). Due to its almost exclusively carbonate catchment, even February values of TCO_2 are relatively high. $\delta^{13}C_{DIC}$ values nearly equal open system carbonate dissolution with soil CO_2, during all seasons.

In contrast, the Zincaghju (II) and the Tagnone River (V) show little seasonal change. Due to excess CO_2, the Tagnone River has 3.5‰ lower $\delta^{13}C_{DIC}$ values than the Zincaghju River. Increased weathering and lower $\delta^{13}C_{DIC}$ values for Corsiglièse and Tagnone River can be attributed to the position of the watersheds. The low altitude and proximity to the sea account for higher mean annual temperatures and increased plant productivity, in comparison to catchments further inland that are located at higher altitudes. This elevates pCO_2 of soils, which in turn lowers $\delta^{13}C_{DIC}$ values.

5.2.3. Lower mixed catchment of the Tavignanu River

Downstream of sample 3 along the Tavignanu River, lithology changes to carbonate bearing rocks. In general, parameter evolution is characterized by mixing with tributary waters of varying composition. For pCO_2, this has almost no influence. Up to sampling point 8, pCO_2 is below or near atmospheric values, during all months. In February, low CO_2 waters even extend down to the mouth. CO_2 from soil and atmosphere are not enough to replenish the amounts that are consumed by carbonate weathering. Between Orta (I) and Vechju River (III) confluence, TCO_2 increases and $\delta^{13}C_{DIC}$ decreases slightly. In this section, soil CO_2 input dominates over atmospheric CO_2 input, thus $\delta^{13}C_{DIC}$ tends to more negative values. In February, TCO_2 is almost stable between sample 6 and 8, where no tributary and presumably no extensive amount of soil water enters along the river course, due to the steep canyon riverbed. Especially in winter, $\delta^{13}C_{DIC}$ values are high because of atmospheric CO_2 influence. This could also be observed during rainwater dominated events of flashy streams (Hagedorn et al., 2016). With increasing temperature in summer, TCO_2 values increase downstream from sample 6, presumably because of evaporation effects. $\delta^{13}C_{DIC}$ values are only affected slightly, because CO_2 evasion is buffered by high HCO_3^-concentrations at ambient pH conditions. Downstream of sample 8, TCO_2 and TA increase, while $\delta^{13}C_{DIC}$ and pH decrease. During winter, when plant activity and soil respiration is low, pCO_2 stays at low levels. In May, July, and October when soil CO_2 production increases at the heavy vegetated, coastal plain, the signal is transferred to the river. pH drops according to rising CO_2 levels, because no CO_2 is consumed by carbonate weathering, due to the dominating siliciclastic lithology.

5.3. pCO_2 and CO_2 transfer

The average value for pCO_2 over the entire main stream was strongly season depended (Fig. 5) with median values from 167 µatm in February to 579 µatm in July (Table 3). These averages are significantly lower compared with reported 1604 to 5479 µatm (sandy soils, Polsenaere and Abril, 2012), 4620/2050 µatm (mean/median, carbonate karst, van Geldern et al., 2015), and 5190 to 10,790 µatm (mixed silicate and carbonate, Khadka et al., 2014). Comparable results of 355 to 398 µatm were reported by Palmer et al. (2001) from a small, high organic, granitic headwater catchment.

The overall CO_2 transfer across the air-water boundary was calculated from F_{CO_2} values and the measures of stream section length and width (Fig. 7). The temporal extrapolation of the four seasonal sample campaigns allowed for the estimation of annual average values for different sections of the Tavignanu River.

In February, initial CO_2 evasion near the source lakes accounted for most of the carbon export from the river. The rest of Tavignanu River remained undersaturated and exhibited minor TCO_2 increases from carbonate weathering and CO_2 uptake from soil and mainly atmosphere. Both pCO_2 and F_{CO_2} median values indicate that the main river is a net sink for atmospheric carbon at this time of the year. Low pCO_2 values are interpreted as a result of reduced plant activity and low temperature in winter. Additionally, increased precipitation rates produce faster surface and subsurface flow, which results in lower resident time of water in soils where it could dissolve CO_2. In May, July, and October, when soil CO_2 contribution increased, upstream CO_2 evasion extends up to Corte (sample 3) and becomes exceedingly strong due to soil CO_2 input and possible in-stream oxidation of organic matter exported from the source lakes. After the city of Corte, most of the CO_2 degasses rapidly, which is enhanced by turbulences of Restonica and Orta River inflow. Between Corte and the coastal plain, CO_2 fluxes are negative or near zero, because water input via tributaries, soil water, and groundwater is limited. This is due to the above mentioned canyon-like riverbed morphology, which results in an almost inert stream. A strong increase in exported CO_2 can be found in the coastal plain where the crops of agricultural areas and strong natural vegetation intensify respiratory CO_2 output into soils, which is then transported into the stream via

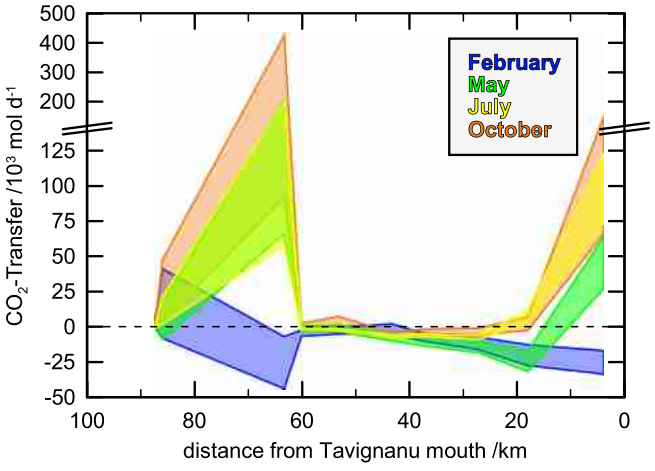

Fig. 7. Downstream evolution of CO_2-Transfer from river water to the atmosphere. Bands depict variance induced by estimation of river width, depth, gas transfer velocities, and error propagation from pCO_2 calculation ($\pm 1\sigma$). Negative values mean CO_2 flux from atmosphere into water.

groundwater discharge. This correlates with the findings of other studies that catchments disturbed by agriculture or other anthropogenic influences exhibit a greater export of old carbon from soils to rivers (Butman et al., 2014; Evans, 2014). Average annual values reflect these trends with (629 ± 234) Mg C yr^{-1} in the high mountains, (−70 ± 12) Mg C yr^{-1} in the low mountain range and canyon part of the Tavignanu River, and (209 ± 63) Mg C yr^{-1} in the coastal plain.

The overall CO_2 budget of the Tavignanu River across the air-water interface is (0.77 ± 0.24) Gg C yr^{-1}. This is about seven times as much as the riverine TCO_2 export to the sea of ca. 0.11 Gg C yr^{-1}.

6. Conclusion

The Tavignanu River catchment combines several environmental parameters, such as an exceptional morphological gradient, lithological diverse sub-catchments, and a pronounced seasonality. Their combinations influence its water chemistry and especially the TCO_2 species. Since the three main streams, namely the Tavignanu, Restonica, and Vechju River, all originate from silicate terrains, TCO_2 values were found to be low when compared to typical carbonate streams. In silicate terrains, most of the TCO_2 originates from soil CO_2 and degenerated organic matter with clear atmospheric influences in winter. Carbonate tributaries derive their TCO_2 mainly from soil and carbonate rock weathering. Seasonal variations correlate with climatic conditions, due to different altitude.

The net carbon budget of the river-atmosphere system for the main channel was subject to seasonal changes. In February, the minor CO_2 evasion around the source area cannot compensate the extensive areas downstream, where pCO_2 remains below atmospheric levels. Hence, the river is a net carbon sink in winter. This characteristic shifts with the warmer season, when plant productivity pumps carbon into the aqueous system. CO_2 evasion in the upstream parts of carbonate-dominated tributaries was not assessed in this study, but presumably play an important role in the total carbon budget of the watershed. This is because small headwater streams from carbonate terrains can show extensive CO_2 export (van Geldern et al., 2015). However, this remains somewhat speculative at this point for high altitude and high relief catchments with rather sparse vegetation. Additionally, several of the smaller tributaries run dry in summer in their upstream parts, which can also influence CO_2 export (von Schiller et al., 2014). Therefore, sampling of carbonate springs of small streams is a reasonable addition for future work for a better integration of the total carbon flux.

In this study, two major influences on the riverine carbon budget could be identified: lithology and seasonal change, which is related to the Mediterranean climate and temperature differences due to high altitude. The Zincaghju, Restonica, and upper Tavignanu River are examples for headwaters in mainly granitic catchments and exhibit water chemistry according to this background. Since 5.7% (Hartmann and Moosdorf, 2012) to 7.2% (Dürr et al., 2005) of the Earth's surface, 9.0% of its high mountain, and 11.4% of its middle mountain ranges (Dürr et al., 2005) consist of acid plutonic rocks, the encountered river water conditions can be transferred to a significant part of the globe. The large abundance of metamorphic rocks in the middle Tavignanu and tributary catchments is met with a global occurrence of metamorphic rocks of 13.0% (Hartmann and Moosdorf, 2012). The other factor, the Mediterranean climate, is found only on 2% of earth's landmass but the impacts of climate change on these regions are discussed intensely. Increased temperature and decreased precipitation will affect aquatic ecosystems particularly in this region (Filipe et al., 2012; Lawrence et al., 2010). This will also have influences on the water supply of the increasing population (294 million in 2000 according to Underwood et al., 2009) that live in areas of Mediterranean climate worldwide. The notable, temporally constant carbon export in the upper catchment consolidates the importance of headwater research for the assessment of global carbon budget estimates (Marx et al., 2017). Altogether, the Tavignanu River is a net CO_2 exporter, however, its exports are minor when compared with other catchments (e.g., Butman and Raymond, 2011; Kanduč et al., 2007; Khadka et al., 2014; Lee et al., 2017; van Geldern et al., 2015). In the context of focus on the atmospheric CO_2 contribution of rivers in numerous studies, these results should encourage a more thorough assessment of riverine carbon budgets. This could be done by continuous high resolution measurement of CO_2 flux and $\delta^{13}C_{DIC}$ with laser spectroscopy, as it is already used for oceanic (Becker et al., 2012), lakes (Attermeyer et al., 2016), volcanic (Rizzo et al., 2014; Rizzo et al., 2015; Schipper et al., 2017), and underground applications (van Geldern et al., 2014). Additionally, upscaling methods to transfer the results to larger areas would probably require a model based approach on CO_2 evasion, such as the model based study of England and Wales (Rawlins et al., 2014), which estimated a CO_2 release of ~65 Gg C yr^{-1}.

Supplementary data to this article can be found online at https://doi.org/10.1016/j.scitotenv.2018.12.158.

Acknowledgements

The authors would like to thank Christian Hanke, Silke Meyer, Lucy Beinert, and Irene Wein (FAU) for help with laboratory analyses and field work. This project was financially supported within the German-French PROCOPE program by the German Academic Exchange Service (DAAD; project-ID 57211614) and the French Ministry of Foreign Affairs (Project No 35374PM). Additional funding was provided by the German Research Foundation (DFG; grant GE 2338/1-1). We thank 3 anonymous reviewers for their constructive and helpful comments.

Declarations of interest

None.

References

Amiotte Suchet, P., Probst, J.L., 1995. A global model for present-day atmospheric/soil CO_2 consumption by chemical erosion of continental rocks (GEM-CO_2). Tellus B 47, 273–280. https://doi.org/10.1034/j.1600-0889.47.issue1.23.x.

Attermeyer, K., Flury, S., Jayakumar, R., Fiener, P., Steger, K., Arya, V., Wilken, F., van Geldern, R., Premke, K., 2016. Invasive floating macrophytes reduce greenhouse gas emissions from a small tropical lake. Sci. Rep. 6, 20424. https://doi.org/10.1038/srep20424.

Aucour, A.-M., Sheppard, S.M.F., Guyomar, O., Wattelet, J., 1999. Use of ^{13}C to trace origin and cycling of inorganic carbon in the Rhône river system. Chem. Geol. 159, 87–105. https://doi.org/10.1016/s0009-2541(99)00035-2.

Aufdenkampe, A.K., Mayorga, E., Raymond, P.A., Melack, J.M., Doney, S.C., Alin, S.R., Aalto, R.E., Yoo, K., 2011. Riverine coupling of biogeochemical cycles between land, oceans, and atmosphere. Front. Ecol. Environ. 9, 53–60. https://doi.org/10.1890/100014.

Barth, J.A.C., Veizer, J., 1999. Carbon cycle in St. Lawrence aquatic ecosystems at Cornwall (Ontario), Canada: seasonal and spatial variations. Chem. Geol. 159, 107–128. https://doi.org/10.1016/s0009-2541(99)00036-4.

Barth, J.A.C., Cronin, A.A., Dunlop, J., Kalin, R.M., 2003. Influence of carbonates on the riverine carbon cycle in an anthropogenically dominated catchment basin: evidence from major elements and stable carbon isotopes in the Lagan River (N. Ireland). Chem. Geol. 200, 203–216. https://doi.org/10.1016/s0009-2541(03)00193-1.

Battin, T.J., Luyssaert, S., Kaplan, L.A., Aufdenkampe, A.K., Richter, A., Tranvik, L.J., 2009. The boundless carbon cycle. Nat. Geosci. 2, 598–600. https://doi.org/10.1038/ngeo618.

Becker, M., Andersen, N., Fiedler, B., Fietzek, P., Körtzinger, A., Steinhoff, T., Friedrichs, G., 2012. Using cavity ringdown spectroscopy for continuous monitoring of δ13C(CO2) and *f*CO2 in the surface ocean. Limnol. Oceanogr. Methods 10, 752–766. https://doi.org/10.4319/lom.2012.10.752.

Brand, W.A., Coplen, T.B., Vogl, J., Rosner, M., Prohaska, T., 2014. Assessment of international reference materials for isotope-ratio analysis (IUPAC technical report). Pure Appl. Chem. 86. https://doi.org/10.1515/pac-2013-1023.

Butman, D.E., Raymond, P.A., 2011. Significant efflux of carbon dioxide from streams and rivers in the United States. Nat. Geosci. 4, 839–842. https://doi.org/10.1038/ngeo1294.

Butman, D.E., Wilson, H.F., Barnes, R.T., Xenopoulos, M.A., Raymond, P.A., 2014. Increased mobilization of aged carbon to rivers by human disturbance. Nat. Geosci. 8, 112. https://doi.org/10.1038/ngeo2322.

Caron, J.M., Bonin, B., 1980. 26° congrès géologique international - Introduction à la géologie du Sud-Est de la France: VI - La Corse. Géologie Alpine. 56, 80–90.

Cartwright, I., 2010. The origins and behaviour of carbon in a major semi-arid river, the Murray River, Australia, as constrained by carbon isotopes and hydrochemistry. Appl. Geochem. 25, 1734–1745. https://doi.org/10.1016/j.apgeochem.2010.08.020.

Cartwright, I., Buick, I.S., 2000. Fluid generation, vein formation and the degree of fluid-rock interaction during decompression of high-pressure terranes: the Schistes

Lustres, Alpine Corsica, France. J. Metamorph. Geol. 18, 607–624. https://doi.org/10.1046/j.1525-1314.2000.00280.x.
Chamberlain, C.P., Waldbauer, J.R., Jacobson, A.D., 2005. Strontium, hydrothermal systems and steady-state chemical weathering in active mountain belts. Earth Planet. Sci. Lett. 238, 351–366. https://doi.org/10.1016/j.epsl.2005.08.005.
Clark, I.D., Fritz, P., 1997. Environmental Isotopes in Hydrogeology. CRC Press/Lewis Publishers, Boca Raton, FL.
Cole, J.J., Prairie, Y.T., Caraco, N.F., McDowell, W.H., Tranvik, L.J., Striegl, R.G., Duarte, C.M., Kortelainen, P., Downing, J.A., Middelburg, J.J., Melack, J., 2007. Plumbing the global carbon cycle: integrating inland waters into the terrestrial carbon budget. Ecosystems 10, 172–185. https://doi.org/10.1007/s10021-006-9013-8.
Coplen, T.B., 2011. Guidelines and recommended terms for expression of stable-isotope-ratio and gas-ratio measurement results. Rapid Commun. Mass Spectrom. 25, 2538–2560. https://doi.org/10.1002/rcm.5129.
Davidson, G.R., 1995. The stable isotopic composition and measurement of carbon in soil CO_2. Geochim. Cosmochim. Acta 59, 2485–2489. https://doi.org/10.1016/0016-7037(95)00143-3.
Deines, P., Langmuir, D., Harmon, R.S., 1974. Stable carbon isotope ratios and the existence of a gas phase in the evolution of carbonate ground waters. Geochim. Cosmochim. Acta 38, 1147–1164. https://doi.org/10.1016/0016-7037(74)90010-6.
Dever, L., Durand, R., Fontes, J.C., Vachier, P., 1983. Etude pedogenetique et isotopique des neoformations de calcite dans un sol sur craie. Geochim. Cosmochim. Acta 47, 2079–2090. https://doi.org/10.1016/0016-7037(83)90033-9.
Doctor, D.H., Kendall, C., Sebestyen, S.D., Shanley, J.B., Ohte, N., Boyer, E.W., 2008. Carbon isotope fractionation of dissolved inorganic carbon (DIC) due to outgassing of carbon dioxide from a headwater stream. Hydrol. Process. 22, 2410–2423. https://doi.org/10.1002/hyp.6833.
Dürr, H.H., Meybeck, M., Dürr, S.H., 2005. Lithologic composition of the Earth's continental surfaces derived from a new digital map emphasizing riverine material transfer. Glob. Biogeochem. Cycles 19. https://doi.org/10.1029/2005gb002515 n/a-n/a.
Duvert, C., Butman, D.E., Marx, A., Ribolzi, O., Hutley, L.B., 2018. CO2 evasion along streams driven by groundwater inputs and geomorphic controls. Nat. Geosci. 11. https://doi.org/10.1038/s41561-018-0245-y.
Egal, E., 1992. Structures and tectonic evolution of the external zone of Alpine Corsica. J. Struct. Geol. 14, 1215–1228. https://doi.org/10.1016/0191-8141(92)90071-4.
Ehleringer, J.R., Cerling, T.E., 2002. C_3 and C_4 photosynthesis. In: Mooney, H.A., Canadell, J.G. (Eds.), Encyclopedia of Global Environmental Change - Volume 2, the Earth System: Biological and Ecological Dimensions of Global Environmental Change. John Wiley & Sons, Chichester, pp. 186–190.
ESRL/GMD, 2016. CO_2 Time Series Data of Monitoring Station Lampedusa, Italy (LMP). National Oceanic and Atmospheric Administration/Earth System Research Laboratory - Global Monitoring Division, Boulder, Colorado, U.S.A.
Evans, C., 2014. Old carbon mobilized. Nat. Geosci. 8, 85. https://doi.org/10.1038/ngeo2334.
Filipe, A.F., Lawrence, J.E., Bonada, N., 2012. Vulnerability of stream biota to climate change in mediterranean climate regions: a synthesis of ecological responses and conservation challenges. Hydrobiologia https://doi.org/10.1007/s10750-012-1244-4.
van Geldern, R., Nowak, M.E., Zimmer, M., Szizybalski, A., Myrttinen, A., Barth, J.A., Jost, H.J., 2014. Field-based stable isotope analysis of carbon dioxide by mid-infrared laser spectroscopy for carbon capture and storage monitoring. Anal. Chem. 86, 12191–12198. https://doi.org/10.1021/ac5031732.
van Geldern, R., Schulte, P., Mader, M., Baier, A., Barth, J.A.C., 2015. Spatial and temporal variations of pCO_2, dissolved inorganic carbon and stable isotopes along a temperate karstic watercourse. Hydrol. Process. 29, 3423–3440. https://doi.org/10.1002/hyp.10457.
Hagedorn, B., Cartwright, I., 2009. Climatic and lithologic controls on the temporal and spatial variability of CO_2 consumption via chemical weathering: an example from the Australian Victorian Alps. Chem. Geol. 260, 234–253. https://doi.org/10.1016/j.chemgeo.2008.12.019.
Hagedorn, B., El-Kadi, A.I., Whittier, R.B., 2016. Controls on the $\delta^{13}C$ DIC and alkalinity budget of a flashy subtropical stream (Manoa River, Hawaii). Appl. Geochem. 73, 49–58. https://doi.org/10.1016/j.apgeochem.2016.07.008.
Halbedel, S., Koschorreck, M., 2013. Regulation of CO_2 emissions from temperate streams and reservoirs. Biogeosciences 10, 7539–7551. https://doi.org/10.5194/bg-10-7539-2013.
Hartmann, J., Moosdorf, N., 2012. The new global lithological map database GLiM: a representation of rock properties at the earth surface. Geochem. Geophys. Geosyst. 13. https://doi.org/10.1029/2012gc004370 n/a-n/a.
Hélie, J.-F., Hillaire-Marcel, C., Rondeau, B., 2002. Seasonal changes in the sources and fluxes of dissolved inorganic carbon through the St. Lawrence River—isotopic and chemical constraint. Chem. Geol. 186, 117–138. https://doi.org/10.1016/s0009-2541(01)00417-x.
Hope, D., Palmer, S.M., Billett, M.F., Dawson, J.J.C., 2004. Variations in dissolved CO_2 and CH_4 in a first-order stream and catchment: an investigation of soil-stream linkages. Hydrol. Process. 18, 3255–3275. https://doi.org/10.1002/hyp.5657.
IPCC, Pachauri, R.K., 2014. In: Meyer, L.A. (Ed.), Climate change 2014: synthesis report. Contribution of working groups I, II and III to the fifth assessment report of the intergovernmental panel on climate change. IPCC, Geneva, Switzerland, p. 151.
Johnson, M.S., Lehmann, J., Riha, S.J., Krusche, A.V., Richey, J.E., Ometto, J.P.H.B., Couto, E.G., 2008. CO_2 efflux from Amazonian headwater streams represents a significant fate for deep soil respiration. Geophys. Res. Lett. 35. https://doi.org/10.1029/2008gl034619.
Kanduč, T., Szramek, K., Ogrinc, N., Walter, L.M., 2007. Origin and cycling of riverine inorganic carbon in the Sava River watershed (Slovenia) inferred from major solutes and stable carbon isotopes. Biogeochemistry 86, 137–154. https://doi.org/10.1007/s10533-007-9149-4.
Kanduč, T., Mori, N., Kocman, D., Stibilj, V., Grassa, F., 2012. Hydrogeochemistry of alpine springs from North Slovenia: insights from stable isotopes. Chem. Geol. 300-301, 40–54. https://doi.org/10.1016/j.chemgeo.2012.01.012.
Kempe, S., 1982. Long-term record of CO_2 pressure fluctuations in fresh waters - Habilitationsschrift. In: Degens, E.T. (Ed.), Transport of Carbon and Minerals in Major World Rivers, Pt 1. 52. Mitt. Geol.-Paläont. Inst. Univ. Hamburg, SCOPE/UNEP Sonderband, Hamburg, pp. 91–332.
Khadka, M.B., Martin, J.B., Jin, J., 2014. Transport of dissolved carbon and CO_2 degassing from a river system in a mixed silicate and carbonate catchment. J. Hydrol. 513, 391–402. https://doi.org/10.1016/j.jhydrol.2014.03.070.
Lauerwald, R., Laruelle, G.G., Hartmann, J., Ciais, P., Regnier, P.A.G., 2015. Spatial patterns in CO_2 evasion from the global river network. Glob. Biogeochem. Cycles 29, 534–554. https://doi.org/10.1002/2014gb004941.
Lawrence, J.E., Lunde, K.B., Mazor, R.D., Bêche, L.A., McElravy, E.P., Resh, V.H., 2010. Long-term macroinvertebrate responses to climate change: implications for biological assessment in mediterranean-climate streams. J. N. Am. Benthol. Soc. 29, 1424–1440. https://doi.org/10.1899/09-178.1.
Lee, K.Y., van Geldern, R., Barth, J.A.C., 2017. A high-resolution carbon balance in a small temperate catchment: insights from the Schwabach River, Germany. Appl. Geochem. 85, 86–96. https://doi.org/10.1016/j.apgeochem.2017.08.007.
Leybourne, M.I., Goodfellow, W.D., 2010. Geochemistry of surface waters associated with an undisturbed Zn–Pb massive sulfide deposit: water–rock reactions, solute sources and the role of trace carbonate. Chem. Geol. 279, 40–54. https://doi.org/10.1016/j.chemgeo.2010.10.002.
Loÿe-Pilot, M.D., Martin, J.M., Morelli, J., 1986. Influence of Saharan dust on the rain acidity and atmospheric input to the Mediterranean. Nature 321, 427–428. https://doi.org/10.1038/321427a0.
Mamane, Y., Dayan, U., Miller, J.M., 1987. Contribution of alkaline and acidic sources to precipitation in Israel. Sci. Total Environ. 61, 15–22. https://doi.org/10.1016/0048-9697(87)90352-4.
Marx, A., Dusek, J., Jankovec, J., Sanda, M., Vogel, T., van Geldern, R., Hartmann, J., Barth, J.A.C., 2017. A review of CO2 and associated carbon dynamics in headwater streams: a global perspective. Rev. Geophys. 55, 560–585. https://doi.org/10.1002/2016rg000547.
Maurice, L., Rawlins, B.G., Farr, G., Bell, R., Gooddy, D.C., 2017. The influence of flow and bed slope on gas transfer in steep streams and their implications for evasion of CO_2. J. Geophys. Res. Biogeosci. 122, 2862–2875. https://doi.org/10.1002/2017jg004045.
Meybeck, M., 1982. Carbon, nitrogen, and phosphorus transport by world rivers. Am. J. Sci. 282, 401–450. https://doi.org/10.2475/ajs.282.4.401.
Mook, W.G., Bommerson, J.C., Staverman, W.H., 1974. Carbon isotope fractionation between dissolved bicarbonate and gaseous carbon dioxide. Earth Planet. Sci. Lett. 22, 169–176. https://doi.org/10.1016/0012-821x(74)90078-8.
Orszag-Sperber, F., Pilot, M.D., 2013. Grands traits du Neogene de Corse. Bull. Soc. Geol. Fr. S7-XVIII, 1183–1187. https://doi.org/10.2113/gssgfbull.S7-XVIII.5.1183.
Palmer, S.M., Hope, D., Billett, M.F., Dawson, J.J.C., Bryant, C.L., 2001. Sources of organic and inorganic carbon in a headwater stream: evidence from carbon isotope studies. Biogeochemistry 52, 321–338. https://doi.org/10.1023/a:1006447706565.
Pawellek, F., Veizer, J., 1994. Carbon cycle in the upper Danube and its tributaries: $\delta^{13}C_{DIC}$ constraints. Isr. J. Earth Sci. 43, 187–194.
Piñol, J., Alcañiz, J.M., Rodà, F., 1995. Carbon dioxide efflux and pCO_2 in soils of three *Quercus ilex* montane forests. Biogeochemistry 30, 191–215. https://doi.org/10.1007/bf02186413.
Plummer, L.N., Busenberg, E., 1982. The solubilities of calcite, aragonite and vaterite in CO_2-H_2O solutions between 0 and 90°C, and an evaluation of the aqueous model for the system $CaCO_3$-CO_2-H_2O. Geochim. Cosmochim. Acta 46, 1011–1040. https://doi.org/10.1016/0016-7037(82)90056-4.
Polsenaere, P., Abril, G., 2012. Modelling CO_2 degassing from small acidic rivers using water pCO_2, DIC and $\delta^{13}C$-DIC data. Geochim. Cosmochim. Acta 91, 220–239. https://doi.org/10.1016/j.gca.2012.05.030.
Rawlins, B.G., Palumbo-Roe, B., Gooddy, D.C., Worrall, F., Smith, H., 2014. A model of potential carbon dioxide efflux from surface water across England and Wales using headwater stream survey data and landscape predictors. Biogeosciences 11, 1911–1925. https://doi.org/10.5194/bg-11-1911-2014.
Raymond, P.A., Bauer, J.E., 2001. Use of ^{14}C and ^{13}C natural abundances for evaluating riverine, estuarine, and coastal DOC and POC sources and cycling: a review and synthesis. Org. Geochem. 32, 469–485. https://doi.org/10.1016/s0146-6380(00)00190-x.
Raymond, P.A., Bauer, J.E., Cole, J.J., 2000. Atmospheric CO_2 evasion, dissolved inorganic carbon production, and net heterotrophy in the York River estuary. Limnol. Oceanogr. 45, 1707–1717. https://doi.org/10.4319/lo.2000.45.8.1707.
Raymond, P.A., Bauer, J.E., Caraco, N.F., Cole, J.J., Longworth, B., Petsch, S.T., 2004. Controls on the variability of organic matter and dissolved inorganic carbon ages in northeast US rivers. Mar. Chem. 92, 353–366. https://doi.org/10.1016/j.marchem.2004.06.036.
Raymond, P.A., Zappa, C.J., Butman, D., Bott, T.L., Potter, J., Mulholland, P., Laursen, A.E., McDowell, W.H., Newbold, D., 2012. Scaling the gas transfer velocity and hydraulic geometry in streams and small rivers. Limnol. Oceanogr. Fluids Environ. 2, 41–53. https://doi.org/10.1215/21573689-1597669.
Raymond, P.A., Hartmann, J., Lauerwald, R., Sobek, S., McDonald, C., Hoover, M., Butman, D., Striegl, R.G., Mayorga, E., Humborg, C., Kortelainen, P., Durr, H., Meybeck, M., Ciais, P., Guth, P., 2013. Global carbon dioxide emissions from inland waters. Nature 503, 355–359. https://doi.org/10.1038/nature12760.
Rizzo, A.L., Jost, H.-J., Caracausi, A., Paonita, A., Liotta, M., Martelli, M., 2014. Real-time measurements of the concentration and isotope composition of atmospheric and volcanic CO_2 at Mount Etna (Italy). Geophys. Res. Lett. 41, 2382–2389. https://doi.org/10.1002/2014GL059722.

Rizzo, A.L., Liuzzo, M., Ancellin, M.A., Jost, H.J., 2015. Real-time measurements of $\delta^{13}C$, CO_2 concentration, and CO_2/SO_2 in volcanic plume gases at Mount Etna, Italy, over 5 consecutive days. Chem. Geol. 411, 182–191. https://doi.org/10.1016/j.chemgeo.2015.07.007.

Rossi, P., Cocherie, A., 1991. Genesis of a Variscan batholith: field, petrological and mineralogical evidence from the Corsica-Sardinia batholith. Tectonophysics 195, 319–346. https://doi.org/10.1016/0040-1951(91)90219-i.

Salomons, W., Mook, W.G., 1986. Isotope geochemistry of carbonates in the weathering zone. In: Fritz, P., Fontes, J.C. (Eds.), The Terrestrial Environment, B - Handbook of Environmental Isotope Geochemistry. 2. Elsevier, pp. 239–269.

von Schiller, D., Marcé, R., Obrador, B., Gómez-Gener, L., Casas-Ruiz, J., Acuña, V., Koschorreck, M., 2014. Carbon dioxide emissions from dry watercourses. Inland Waters 4, 377–382. https://doi.org/10.5268/iw-4.4.746.

Schipper, C.I., Moussallam, Y., Curtis, A., Peters, N., Barnie, T., Bani, P., Jost, H.J., Hamilton, D., Aiuppa, A., Tamburello, G., Giudice, G., 2017. Isotopically ($\delta^{13}C$ and $\delta^{18}O$) heavy volcanic plumes from central Andean volcanoes: a field study. Bull. Volcanol. 79, 65. https://doi.org/10.1007/s00445-017-1146-4.

Sharp, M., Tranter, M., Brown, G.H., Skidmore, M., 1995. Rates of chemical denudation and CO_2 drawdown in a glacier-covered alpine catchment. Geology 23, 61. https://doi.org/10.1130/0091-7613(1995)023<0061:rocdac>2.3.co;2.

Shin, W.J., Chung, G.S., Lee, D., Lee, K.S., 2011. Dissolved inorganic carbon export from carbonate and silicate catchments estimated from carbonate chemistry and $\delta^{13}C_{DIC}$. Hydrol. Earth Syst. Sci. 15, 2551–2560. https://doi.org/10.5194/hess-15-2551-2011.

Telmer, K., Veizer, J., 1999. Carbon fluxes, pCO_2 and substrate weathering in a large northern river basin, Canada: carbon isotope perspectives. Chem. Geol. 159, 61–86. https://doi.org/10.1016/s0009-2541(99)00034-0.

Tranvik, L.J., Downing, J.A., Cotner, J.B., Loiselle, S.A., Striegl, R.G., Ballatore, T.J., Dillon, P., Finlay, K., Fortino, K., Knoll, L.B., Kortelainen, P.L., Kutser, T., Larsen, S., Laurion, I., Leech, D.M., McCallister, S.L., McKnight, D.M., Melack, J.M., Overholt, E., Porter, J.A., Prairie, Y., Renwick, W.H., Roland, F., Sherman, B.S., Schindler, D.W., Sobek, S., Tremblay, A., Vanni, M.J., Verschoor, A.M., von Wachenfeldt, E., Weyhenmeyer, G.A., 2009. Lakes and reservoirs as regulators of carbon cycling and climate. Limnol. Oceanogr. 54, 2298–2314. https://doi.org/10.4319/lo.2009.54.6_part_2.2298.

Underwood, E.C., Viers, J.H., Klausmeyer, K.R., Cox, R.L., Shaw, M.R., 2009. Threats and biodiversity in the mediterranean biome. Divers. Distrib. 15, 188–197. https://doi.org/10.1111/j.1472-4642.2008.00518.x.

Ward, N.D., Bianchi, T.S., Medeiros, P.M., Seidel, M., Richey, J.E., Keil, R.G., Sawakuchi, H.O., 2017. Where carbon Goes when water flows: carbon cycling across the aquatic continuum. Front. Mar. Sci. 4. https://doi.org/10.3389/fmars.2017.00007.

Wehrli, B., 2013. Biogeochemistry: conduits of the carbon cycle. Nature 503, 346–347. https://doi.org/10.1038/503346a.

Wetzel, R.G., 1992. Gradient-dominated ecosystems: sources and regulatory functions of dissolved organic matter in freshwater ecosystems. Hydrobiologia 229, 181–198. https://doi.org/10.1007/bf00007000.

Wetzel, R.G., 2001. Limnology. Third edition. Academic Press, San Diego.

Wolf-Gladrow, D.A., Zeebe, R.E., Klaas, C., Körtzinger, A., Dickson, A.G., 2007. Total alkalinity: the explicit conservative expression and its application to biogeochemical processes. Mar. Chem. 106, 287–300. https://doi.org/10.1016/j.marchem.2007.01.006.

Yang, C., Telmer, K., Veizer, J., 1996. Chemical dynamics of the "St. Lawrence" riverine system: δD_{H2O}, $\delta^{18}O_{H2O}$, $\delta^{13}C_{DIC}$, $\delta^{34}S_{sulfate}$, and dissolved $^{87}Sr/^{86}Sr$. Geochim. Cosmochim. Acta 60, 851–866. https://doi.org/10.1016/0016-7037(95)00445-9.